Antiviral Research 169 (2019) 104558

Contents lists available at ScienceDirect

Antiviral Research

journal homepage: www.elsevier.com/locate/antiviral

The ReFRAME library as a comprehensive drug repurposing library to identify mammarenavirus inhibitors

Yu-Jin Kim[a], Beatrice Cubitt[a], Emily Chen[b], Mitchell V. Hull[b], Arnab K. Chatterjee[b], Yingyun Cai[c], Jens H. Kuhn[c], Juan C. de la Torre[a,*]

[a] *Department of Immunology and Microbiology, The Scripps Research Institute, La Jolla, CA, 92037, USA*
[b] *California Institute for Biomedical Research, La Jolla, CA, 92037, USA*
[c] *Integrated Research Facility at Fort Detrick (IRF-Frederick), National Institute of Allergy and Infectious Diseases (NIAID), National Institutes of Health (NIH), B-8200 Research Plaza, Fort Detrick, Frederick, MD, 21702, USA*

ARTICLE INFO

Keywords:
Mammarenavirus
Antiviral drugs
ReFRAME library
Screen
Lassa virus
LCMV

ABSTRACT

Several mammarenaviruses, chiefly Lassa virus (LASV) in Western Africa and Junín virus (JUNV) in the Argentine Pampas, cause severe disease in humans and pose important public health problems in their endemic regions. Moreover, mounting evidence indicates that the worldwide-distributed mammarenavirus lymphocytic choriomeningitis virus (LCMV) is a neglected human pathogen of clinical significance. The lack of licensed mammarenavirus vaccines and partial efficacy of current anti-mammarenavirus therapy limited to an off-label use of the nucleoside analog ribavirin underscore an unmet need for novel therapeutics to combat human pathogenic mammarenavirus infections. This task can be facilitated by the implementation of "drug repurposing" strategies to reduce the time and resources required to advance identified antiviral drug candidates into the clinic. We screened a drug repurposing library of 11,968 compounds (Repurposing, Focused Rescue and Accelerated Medchem [ReFRAME]) and identified several potent inhibitors of LCMV multiplication that had also strong anti-viral activity against LASV and JUNV. Our findings indicate that enzymes of the rate-limiting steps of pyrimidine and purine biosynthesis, the pro-viral MCL1 apoptosis regulator, BCL2 family member protein and the mitochondrial electron transport complex III, play critical roles in the completion of the mammarenavirus life cycle, suggesting they represent potential druggable targets to counter human pathogenic mammarenavirus infections.

1. Introduction

As mammarenaviruses cause chronic infections of, primarily, rodents, these viruses have a worldwide distribution. Human infections occur through mucosal exposure to aerosols, or by direct contact of abraded skin with infectious materials (Buchmeier et al., 2007). Several mammarenaviruses cause severe disease in humans and pose important public health problems in their endemic regions (Buchmeier et al., 2007; Enria et al., 2008; Geisbert and Jahrling, 2004; McCormick and Fisher-Hock, 2002; Peters, 2002). The Old World mammarenavirus Lassa virus (LASV) is highly prevalent in Western Africa where it causes Lassa fever (LF), a disease associated with high morbidity and significant lethality in patients who develop severe symptoms (Gunther and Lenz, 2004). LASV is estimated to infect several hundred thousand people yearly. Notably, increased travel has resulted in cases of LF in non-endemic metropolitan areas including the US (Freedman and Woodall, 1999; Isaacson, 2001). Likewise, the New World (NW) mammarenavirus Junín virus (JUNV) causes Argentinian hemorrhagic fever (AHF), a severe illness (lethality of 15–30%) endemic to the Argentine Pampas characterized by hemorrhagic and neurological manifestations (Peters, 2002). Moreover, several mammarenaviruses, including LASV and JUNV, pose credible biodefense concerns (Borio et al., 2002). In addition, mounting evidence indicates that the worldwide-distributed mammarenavirus lymphocytic choriomeningitis virus (LCMV) is a neglected human pathogen of clinical significance (Barton et al., 2002; Fischer et al., 2006; Jahrling and Peters, 1992; Palacios et al., 2008; Peters, 2006).

Concerns posed by human pathogenic mammarenaviruses are exacerbated by the lack of licensed arenavirus vaccines and drawbacks of current anti-mammarenavirus therapy. Such therapy is limited to off-label use of ribavirin (Rib) that is only partially effective, has a narrow therapeutic window and is associated with side effects (Damonte and

---

[*] Corresponding author.
E-mail address: juanct@scripps.edu (J.C. de la Torre).

https://doi.org/10.1016/j.antiviral.2019.104558
Received 21 May 2019; Received in revised form 9 July 2019; Accepted 11 July 2019

0166-3542/

Coto, 2002; Moreno et al., 2011; Parker, 2005). Several compounds have been reported to have anti-mammarenaviral activity in cultured cells, but their safety and efficacy remain to be determined (Lee et al., 2011). However, the broad-spectrum antiviral favipiravir (a.k.a. T-705) (Gowen et al., 2013; Mendenhall et al., 2011a, 2011b; Safronetz et al., 2015) and the mammarenaviral glycoprotein (GP)-mediated fusion inhibitor ST-193 (Cashman et al., 2011) have yielded very promising results in different animal models of mammarenaviral disease. Nevertheless, the identification and characterization of safe and effective anti-mammarenaviral drugs can facilitate the implementation of combination therapy to combat human pathogenic mammarenavirus infection, an approach known to counteract the emergence of drug resistant variants often observed with monotherapy strategies.

Drug repurposing strategies can significantly reduce the time and resources required to advance a candidate antiviral drug into the clinic. These advantages are particularly relevant for emerging viral diseases, as limited market opportunities are an obstacle for the development and licensing of new drugs. Existing knowledge about medicinal chemistry, pharmacology, and toxicology of the repurposed candidate drug will minimize the labor and resource-intensive efforts involved in preclinical optimization of newly discovered hits in traditional drug-discovery approaches (Ashburn and Thor, 2004; Pushpakom et al., 2019). Moreover, drug repurposing can generate new knowledge in virus biology by uncovering previously unexplored pathways and specific host cell factors contributing to different steps of the virus "life" cycle. This knowledge can be harnessed to identify new targets and therapeutics.

Here, we document the screening of the Repurposing, Focused Rescue and Accelerated Medchem (ReFRAME) library (Janes et al., 2018) for compounds with anti-LCMV activity. Screening of 11,968 compounds in the library identified 109 primary hits, of which 23 were confirmed. We selected ten confirmed hits that exhibited potent dose-dependent anti-LCMV activities and selectivity index (SI) values > 20 for follow-up studies. We used established cell-based assays (Emonet et al., 2009; Lee et al., 2002; Pinschewer et al., 2003; Rojek et al., 2008; Urata et al., 2012; Vazquez-Calvo et al., 2013) to examine the effect of selected hits (SI > 20) on different steps of the LCMV life cycle. Seven hits interfered with a post-virion cell entry step and targeted the activity of the virus ribonucleoprotein complex (vRNP) responsible for directing viral RNA replication and gene transcription. These hits included inhibitors of inosine monophosphate dehydrogenase (IMPDH) involved in purine biosynthesis and inhibitors of dihydroorotate dehydrogenase (DHODH) and uridine monophosphate synthetase (UMPS) enzymes involved in pyrimidine biosynthesis. In addition, inhibitors of the pro-viral MCL1 apoptosis regulator, BCL2 family member (MCL1) protein and the mitochondrial electron transport complex (mETC) III also exhibited strong anti-LCMV activity. Several tested hits also had potent antiviral activity against LASV and JUNV. Our findings have uncovered host cell factors and pathways involved in the completion of the mammarenavirus replication cycle that can be explored as potential targets for the development of antiviral drugs against human pathogenic mammarenaviruses.

2. Materials and methods

2.1. Chemical library

The ReFRAME (Repurposing, Focused Rescue, and Accelerated Medchem) library built at the California Institute for Biomedical Research (Calibr) (Janes et al., 2018) is a best-in-class drug repurposing collection for fast-track drug discovery. Approximately 12,000 high-value compounds are available for screening from a total set of ≈15,000 entries from three commercial drug databases. This library contains purchased or resynthesized US Food and Drug Administration (FDA)-approved/registered drugs (≈35%) and investigational new drugs (INDs). These INDs are currently or previously in any phase of clinical development (≈65%), including > 1000 non-commercially available compounds with non-disclosed structures. Structures were manually determined using broad competitive intelligence resources. The scale and comprehensiveness of the Calibr's drug repurposing library is greater than typical FDA-approved drug libraries.

2.2. Cells and viruses

Grivet (*Chlorocebus aethiops*) Vero (ATCC #CCL-81), human A549 (ATCC CCL-185) and human 293T (ATCC CRL-3216) cells were maintained in Dulbecco's modified eagle medium (DMEM) (Thermo Fisher Scientific, Waltham, MA) containing 10% heat inactivated fetal bovine serum (FBS), 2 mM of L-glutamine, 100 mg/ml of streptomycin, and 100 U/ml of penicillin. MCL1 knock-out mouse embryonic fibroblasts (MEF/MCL1-KO) and MEF/MCL1-KO reconstituted with a lentivirus expressing MCL1 (MEF/MCL1) (Ohmer et al., 2016) were maintained in DMEM containing 10% FBS, 2 mM of L-Glutamine, 100 mg/ml of streptomycin, 100 U/ml of penicillin, and 50 μM of 2-mercaptoethanol. The tri-segmented form of the live attenuated vaccine strain Candid#1 of JUNV expressing green fluorescent protein (GFP, r3Can/GFP) (Emonet et al., 2011), recombinant LCMV expressing GFP (rLCMV/GFP-P2A-NP, here referred to as rLCMV/GFP) (Miranda et al., 2018), rLCMV expressing *Zoanthus* sp. green fluorescent protein (ZsGreen, ZsG) (rLCMV/ZsG-P2A-NP, referred to as rLCMV/ZsG) (Iwasaki et al., 2018), a single cycle infectious rLCMV expressing ZsG (rLCMVΔGPC/ZsG-P2A-NP, here referred to as rLCMVΔGPC/ZsG) (Iwasaki et al., 2018), a wild-type LCMV-Armstrong (WT-LCMV), and LASV-Josiah expressing GFP (rLASV/GFP) (Cai et al., 2018) have been described. Vesicular stomatitis Indiana virus (VSIV) was grown and titrated as described (Giachetti and Holland, 1989).

2.3. Cell cytotoxicity assay and CC_{50} determination

Cell viability was assessed using the CellTiter 96 AQueous One Solution reagent (Promega, Madison, WI; CAT #: G3580). This method determines the number of viable cells based on conversion of formazan product from 3-(4,5-dimethylthazol-2-yl)-5-(3-carboxymethoxyphenyl)-2-(4-sulfophenyl)-2H-tetrazolim (MTS) by nicotinamide adenine dinucleotide phosphate (NADPH) or nicotinamide adenine dinucleotide phosphate (NADH) generated in living cells. A549 cells were plated on a 96-well clear bottom plate (2.0 x 10^4 cells/well) 1 day before drug treatment. Serial dilutions (3-fold) of each compound were added and incubated at 37 °C and 5% CO_2. At 48 h after drug treatment, CellTiter 96 AQueous One solution reagent (Promega) was added and incubated for 15 min at 37 °C and 5% CO_2. The absorbance was measured at 490 nm by using an enzyme-linked immunosorbent assay (ELISA) reader (SPECTRA max plus 384, Molecular Devices, Sunnyvale, CA). The resulting optical densities were normalized with dimethylsulfoxide (DMSO) vehicle control group, which was adjusted to 100%. Half maximal cytotoxic concentrations (CC_{50}) were determined using GraphPad Prism.

2.4. Viral growth kinetics and EC_{50} determination

For growth kinetics, cells (M24-well plate) were infected at the indicated MOI and in the presence of the indicated compound concentration. At the indicated hours post-infection (h pi), tissue-culture supernatants (TCS) were collected, and viral titers determined by indirect immunofluorescence assay (Battegay, 1993).

For determination of compounds' EC_{50}, cells were plated on 96-well clear-bottom black plates (2.0 x 10^4 cells/well) and incubated for 20 h at 37 °C and 5% CO_2. Cells were pre-treated 2 h before infection with 3-fold serial dilutions of each compound. Cells were infected (MOI = 0.01) with rLCMV/ZsG-P2A-NP in the presence of the compounds. At 48 h pi, cells were fixed with 4% paraformaldehyde (PFA). ZsG expression was determined by fluorescence using a fluorescent plate reader (Synergy H4 Hybrid Multi-Mode Microplate Reader, BioTek, Winooski, VT). Mean relative fluorescence units were normalized with vehicle control group (DMSO), which was adjusted to 100%. ZsG expression was normalized for total cell protein in the lysate (Pierce BCA Protein Assay Kit, Thermo Scientific, #23227). Half maximal effective concentrations (EC_{50}s) were determined using GraphPad Prism. The selectivity indexes (SIs) for hit compounds were determined using the ratio CC_{50}/EC_{50}.

2.5. LCMV minigenome assay

The LCMV minigenome (MG) assay was performed as described (Perez et al., 2003). Briefly, 293T cells were cultured on poly-L-lysine-coated M-12 well plates (4.5 x 10^5 cells/well) 1 d before transfection. Cells were transfected with a set of plasmids containing 0.5 µg of cytomegalovirus T7 polymerase promoter (pC-T7), 0.5 µg of pMG-chloramphenicol acetyl transferase (CAT) reporter, 0.3 µg of pC-NP, and 0.3 µg of pC-L using lipofectamine 2000 (2.5 µl/µg of DNA) (Thermo Fisher Scientific, Waltham, MA). After 5 h, transfection mixture was replaced with fresh medium containing each selected hit compound and incubated for 72 h at 37 °C and 5% CO_2. At 72 h post-transfection, whole cell lysates were harvested to determine expression of CAT using CAT ELISA kit (product number 11363727001; Roche, Sydney, Australia). Briefly, whole cell lysates were prepared with 0.5 ml of lysis buffer, and 10 µl of each sample were used for the reaction. Diluted samples were added onto CAT ELISA plates and incubated for 1 h at 37 °C. After incubation with samples, plates were washed, and primary antibody (anti-CAT-digoxigenin [DIG]) and secondary antibody (anti-DIG-peroxidase [POD]) were added sequentially followed by the substrate. After 20-min, absorbance was measured using the ELISA reader at 405 nm for samples and 490 nm for the reference.

2.6. Budding assay

The luciferase-based budding assay was performed as described (Capul and de la Torre, 2008). Briefly, 293T cells were plated on poly-L-lysine-coated M-12 well plates (3.5 x 10^5 cells/well). After overnight incubation, 2 µg of DNA of either pC-LASV-Z-*Gaussia* luciferase (GLuc) or pC-LASV-mutant Z[G2A]-GLuc was transfected using Lipofectamine 2000 (2.5 µl/µg of DNA). After 5 h, the transfection mixture was replaced with fresh medium containing the indicated hit compound. After 48 h, TCS containing virion-like particles (VLPs) were harvested and clarified by low-speed centrifugation to remove cell debris. Aliquots (20 µl each) from TCS samples were added to 96-well black plates (VWR, West Chester, PA), and 50 µl of SteadyGlo luciferase reagent (Promega, Madison, WI) was added to each well. Whole cell lysates (WCL) from the same samples were processed to determine cell-associated activity (relative light units) of GLuc. The luminescence signal was measured by the Berthold Centro LB 960 luminometer (Berthold Technologies, Oak Ridge, TN). Activity of GLuc in TCS and WCL were used as surrogates of Z expression. Budding efficiency was defined as the ratio $Z_{VLP}/Z_{VLP}+Z_{WCL}$.

2.7. Virus titration

Virus titers of rLCMV/GFP, rLCMV/ZsG, rLCMVΔGPC/ZsG and WT-LCMV were determined by focus-forming assay (Battegay, 1993). Serial dilutions of samples (10-fold) were used to infect Vero cell monolayers in a 96-well plate. At 20 h pi, cells were fixed with 4% PFA in phosphate-buffered saline (PBS). Foci of rLCMV/GFP, rLCMV/ZsG, and rLCMVΔGPC/ZsG, were determined by epifluorescence. Foci of WT-LCMV were revealed by using the rat monoclonal antibody VL4 to NP conjugated to Alexa Fluor 488. Vesicular stomatitis Indiana virus (VSIV), wild-type LASV (Josiah strain) and rLASV/GFP titers were determined by plaque assay as described (Cai et al., 2018). Briefly, cells were infected with 10-fold serial dilutions. After 90 min, virus inocula were aspirated, and an agarose overlay (complete 1x minimum essential media containing 2% FBS and 0.9% agarose) was added. At 24 h pi, cells were fixed (10% formaldehyde), agarose overlays were removed, and cells were stained with 0.1% crystal violet solution.

2.8. Reverse transcriptase-polymerase chain reaction

A549 cells were infected with rLCMV/ZsG-P2A-NP in the presence (5 µM) of AVN-944 or brequinar (BQN), or vehicle control DMSO. Total RNA was isolated using Tri Reagent (Invitrogen, Carlsbad, CA) according to the manufacturer's instruction. Total RNA (5 µg) was reversely transcribed to cDNA using SuperScript™ IV First-Strand Synthesis System (Thermo Fisher Scientific, Waltham, MA). Then, semi-quantitative reverse transcriptase-polymerase chain reaction (RT-PCR) was performed using LCMV NP-specific primers (forward 5′-ATGCAGTCCATGAGTGCACAGT-3’; reverse 5′-CTCAGAAGTCTCAACCAGACTG-3′) and glyceraldehyde 3-phosphate dehydrogenase (GAPDH)-specific primers (forward 5′-TGACATCAAGAAGGTGGTGAAGCAG-3’; reverse 5′-ATTGTCATACCAGGAAATGAGCTTGAC-3′).

2.9. Biosafety

Experiments involving the use of rLASV/GFP and LASV-Josiah were performed under maximum containment/biosafety level 4 (BSL-4) conditions in the BSL-4 suites of the NIH/NIAID/DCR Integrated Research Facility at Fort Detrick (IRF-Frederick) (Jahrling et al., 2014) following approved standard operating procedures (Janosko et al., 2016; Mazur et al., 2016).

3. Results

3.1. Screening of the ReFRAME library for inhibitors of LCMV multiplication

We screened 11,968 compounds from the ReFRAME library (Janes et al., 2018) using a described cell-based infection assay tracking the expression of the reporter gene GFP expressed by rLCMV/GFP (Miranda et al., 2018) (Fig. 1A). The primary screen was done at a single (10 µM) drug concentration. Each plate included rLCMV/GFP-infected Vero E6 cells treated with Rib (200 µM), a validated inhibitor of LCMV multiplication, and vehicle control (VC = 0.1% DMSO). To account for possible plate effects, we incorporated the Rib and VC controls in columns 1 and 24. We used maximum (VC) and minimal (Rib) GFP signals from columns 1 and 24 of each plate to generate Z’ scores (Fig. 1B), which showed high consistency on assay performance among plates. Primary hits were selected based on the following criteria: 1) > 50% inhibition of GFP expression, and 2) low toxicity (cell biomass > 60%, as determined by 4′,6-diamidino-2-phenylindole (DAPI) staining) compared to that observed from VC-treated and infected cells (no compounds). We selected primary hits (N = 109) based on inhibition (> 50%) of GFP expression in rLCMV/GFP-infected (MOI = 0.01) cells at 48 h pi. We retested primary hits in a repeat experiment using triplicates for each hit at a single concentration (10 µM) and confirmed 23 hits (Supplemental Fig. 1). These 23 hits inhibited multiplication of both rLCMV/GFP and a different rLCMV expressing the ZsG reporter gene (rLCMV/ZsG) with similar efficiency.

3.2. Dose-dependent effect of confirmed selected hits

We selected the ten confirmed hits with the highest LCMV inhibitory effect in the confirmation test for further studies. We first examined their dose-dependent effect on rLCMV/ZsG multiplication in A549 cells (Fig. 2). We treated cells with 3-fold serial dilutions of each compound starting 2 h prior to infection (MOI = 0.01) with rLCMV/ZsG and maintained compounds throughout the course of infection. We also examined the dose-dependent effect of confirmed hits on cell viability

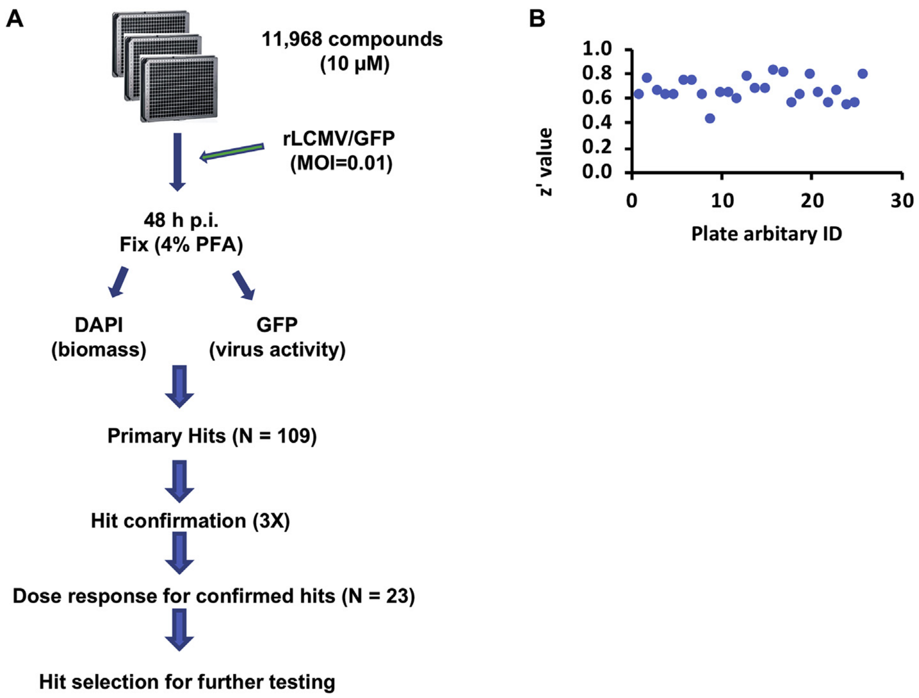

Fig. 1. (A) Screening outline. Compounds (30 nL of 10 mM stocks), Rib (60 nL of 100 mM stock), and dimethyl sulfoxide vehicle control (30 nL) were dispensed onto 384-well black clear-bottom plates using Echo® Acoustic Liquid dispenser. Vero cells were infected (MOI = 0.01) with rLCMV/GFP. At 1 h pi, single cell preparations were made, and 1 x 10^4 cells/well were seeded in 30 μl of media (DMEM with 10% FBS). At 48 h pi, cells were fixed by adding 30 μl of 8% PFA in PBS. After 30 min, cells were washed with PBS, and stained with DAPI. Relative GFP and DAPI fluorescent units were measured using Advanced Hybrid microplate reader Synergy H4. Primary screen was done at a single compound concentration (10 μM). Primary hits were confirmed in triplicate, and a dose response assay confirmed hits. (B) For each plate the Z′ score was calculated by using maximum (DMSO vehicle control [VC]) and minimal (ribavirin [Rib]) GFP signals.

using CellTiter 96 AQueous One Solution reagent. ZsG expression (virus multiplication) was normalized by assigning a value of 100% to ZsG expression in VC-treated and infected cells. Formazan production (cell viability), determined by ELISA, was normalized by assigning a value of 100% cell viability to VC-treated cells. We used these normalized values to determine the EC_{50} and CC_{50} values for the different compounds and ranked them based on their SI (Fig. 2M). As references, we also determined under the same experimental conditions EC_{50} and CC_{50} values for Rib and favipiravir.

3.3. Steps of the LCMV replication cycle affected by selected inhibitors

To gain insights about the mechanisms by which selected hits exerted their anti-LCMV activity, we examined the effect of these compounds on distinct steps of the LCMV replication cycle. We first examined whether the compounds affected a cell entry or post-cell entry step of the LCMV replication cycle. We performed a time-of-addition experiment in which compounds were added 2 h prior infection or 2 h pi (Fig. 3A). We used the single cycle infectious rLCMVΔGPC/ZsG, which eliminated the need for NH_4Cl treatment to prevent the confounding factor introduced by multiple rounds of infection (Rodrigo et al., 2011). All tested compounds, except antimycin A, exhibited a similar robust (≥80%) degree of inhibition of rLCMVΔGPC/ZsG infection, as determined by ZsG expression, when added 2 h prior to or 2 h pi, whereas antimycin A exerted a lower level (20–40%) of inhibition. However, antimycin A exhibited a robust anti-LCMV effect in a cell-based infection assay (Fig. 2A). These apparent discrepancies may reflect differences between experimental conditions involving multiple rounds of infection (Fig. 2A) and one single round of infection (Fig. 3A). To examine whether reduced expression of ZsG correlated with reduced viral RNA synthesis, we used an LCMV MG assay that mimics the biosynthetic processes of RNA replication and gene transcription directed by the virus polymerase complex (Iwasaki and de la Torre, 2018; Iwasaki et al., 2018; Vazquez-Calvo et al., 2013). All the hits tested inhibited (5 μM) LCMV MG activity, as measured by CAT expression (Fig. 3B).

We next examined the effect of the compounds on LCMV budding, a process that is directed by the mammarenaviral Z matrix protein (Perez et al., 2003; Urata et al., 2012). We transfected cells with a Z-expressing plasmid and quantified Z protein levels in whole cell lysates (Z_{WCL}) and virus like particles (Z_{VLP}) collected from TCS of transfected cells (Urata et al., 2012). None of the tested compounds exhibited a significant effect on Z budding efficiency (Fig. 3C).

3.4. Effects of representative compounds on propagation, RNA synthesis, and production of infectious progeny of LCMV

We selected two hit compounds, AVN-944 and brequinar (BQN), to examine their effects on cell-to-cell propagation, RNA synthesis, and production of infectious LCMV progeny over time (Fig. 4). A549 cells were infected with rLCMV/ZsG in the presence (5 μM) of each compound and, at the indicated times pi, numbers of virus-infected cells (Fig. 4A), semiquantitative levels of synthesis of viral RNA (Fig. 4B) and production of cell-free infectious viral progeny (Fig. 4C) were determined. Both compounds strongly inhibited LCMV cell-to-cell propagation, which correlated with reduced viral RNA synthesis and production of infectious progeny. To confirm that the hit compounds exhibited similar antiviral activity against wild-type (WT) LCMV and rLCMV expressing reporter genes, we examined the effect of BQN on production of infectious WT-LCMV (Fig. 4D) and viral RNA synthesis (Fig. 4E).

3.5. Effects of pyrimidine biosynthesis inhibitors on LCMV propagation in interferon (IFN) deficient cells

Antiviral activity of pyrimidine biosynthesis inhibitors may be mediated by their ability to enhance the host cell type I and III IFN response rather than a direct effect of these inhibitors on virus multiplication (Lucas-Hourani et al., 2013). Likewise, at least some pyrimidine biosynthesis inhibitors can induce a type I IFN-independent antiviral state (Chung et al., 2016; Luthra et al., 2018). The four screened pyrimidine biosynthesis inhibitors we tested (azaribine, azauridine, BQN and pyrazofurin) had similar anti-LCMV activity in IFN-competent (A549) and IFN-deficient (Vero E6) cells (Fig. 5A). In addition, the type I IFN-induced antiviral state in Vero E6 cells effectively restricted VSIV, but not LCMV, multiplication (Fig. 5B and C). These findings indicated that the anti-LCMV activity of these compounds was not likely mediated by the induction of antiviral gene

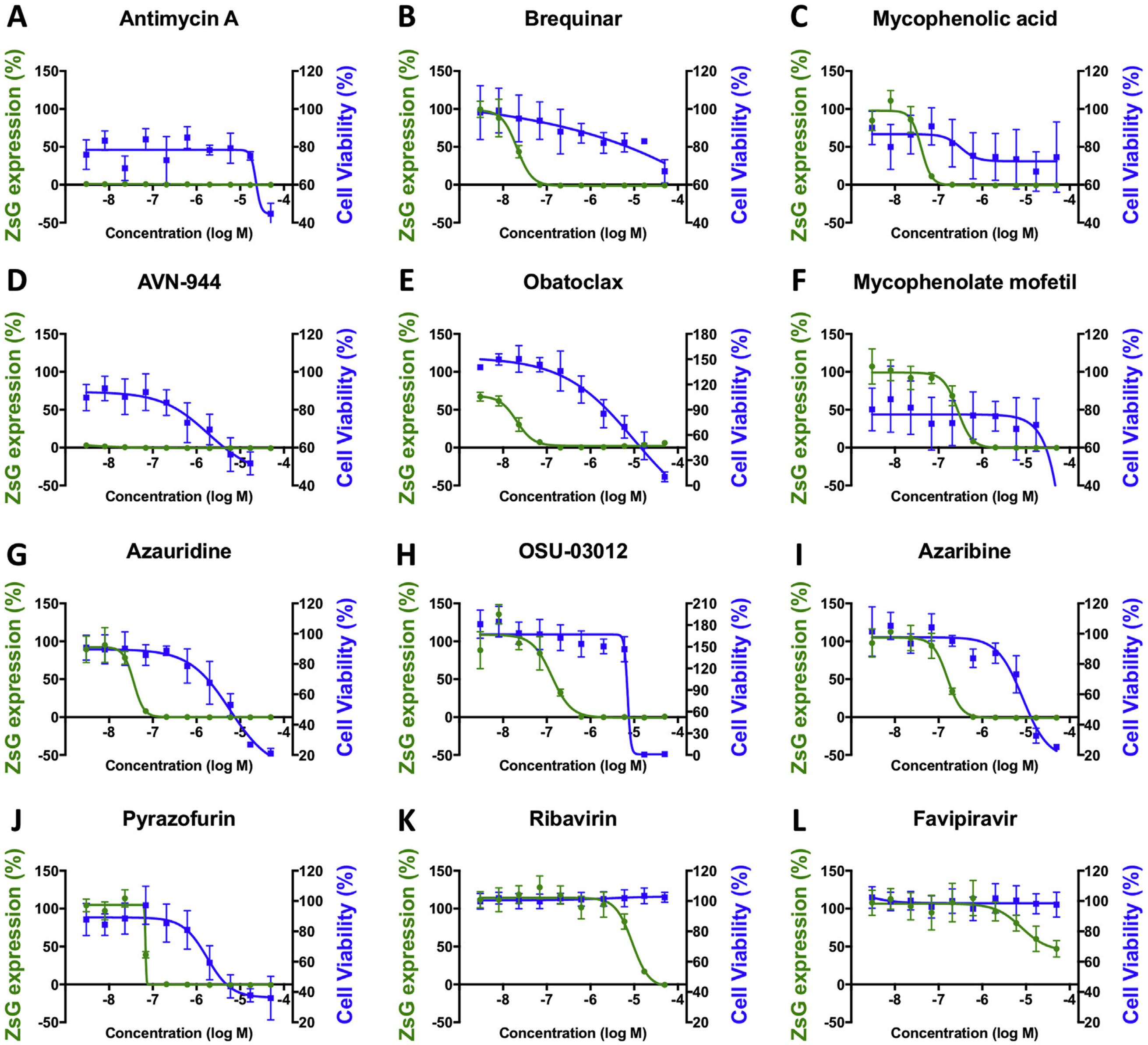

M

Hit compound	CC_{50} (μM)	EC_{50} (μM)	SI
Antimycin A	22.961	<0.003	>7653.851
Brequinar	>50.000	0.021	>2404.363
Mycophenolic acid	>50.000	0.040	>1247.384
AVN-944	1.862	<0.003	>620.698
Obatoclax	9.954	0.020	490.908
Mycophenolate mofetil	48.641	0.274	177.828
Azauridine	5.781	0.037	158.125
OSU-03012	7.063	0.130	54.200
Azaribine	8.395	0.158	53.088
Pyrazofurin	1.742	0.068	25.586
Ribavirin (Control)	>200	9.036	>22.132
Favipiravir (Control)	>200	7.889	>25.353

(caption on next page)

Fig. 2. Dose-dependent effect of selected hit compounds on LCMV multiplication. (A-L) Inhibitory effect of selected hit compounds on LCMV propagation and cell viability. For viral inhibition test, A549 cells were pre-treated with serially diluted compound solutions for 2 h before inoculation with rLCMV/ZsG) (MOI = 0.01). At 48 h pi, fluorescence intensities (relative fluorescent units) were measured. For cell viability assay, serially diluted compounds were added to cells, and cell cytotoxicity was determined 48 h later. Data were normalized to VC (DMSO)-treated group, which was adjusted to 100%. (M**)** Summary of 50% cytotoxic concentration (CC_{50}), 50% inhibitory concentration (EC_{50}), and selectivity index (SI).

components of the host cell innate defense mechanisms.

3.6. Effect of selected hits on multiplication of the LASV and JUNV

We examined the effect of five compounds with anti-LCMV activity: AVN-944, BQN, mycophenolic acid (MPA), obatoclax (OLX), and pyrazofurin (PYF) on multiplication of the HF-associated mammarenavirus LASV (Fig. 6A). A549 cells were infected at a MOI = 0.1 with rLASV/GFP (Cai et al., 2018) and treated with these compounds. At 48 h pi, cells were fixed, and virus multiplication was assessed based on GFP

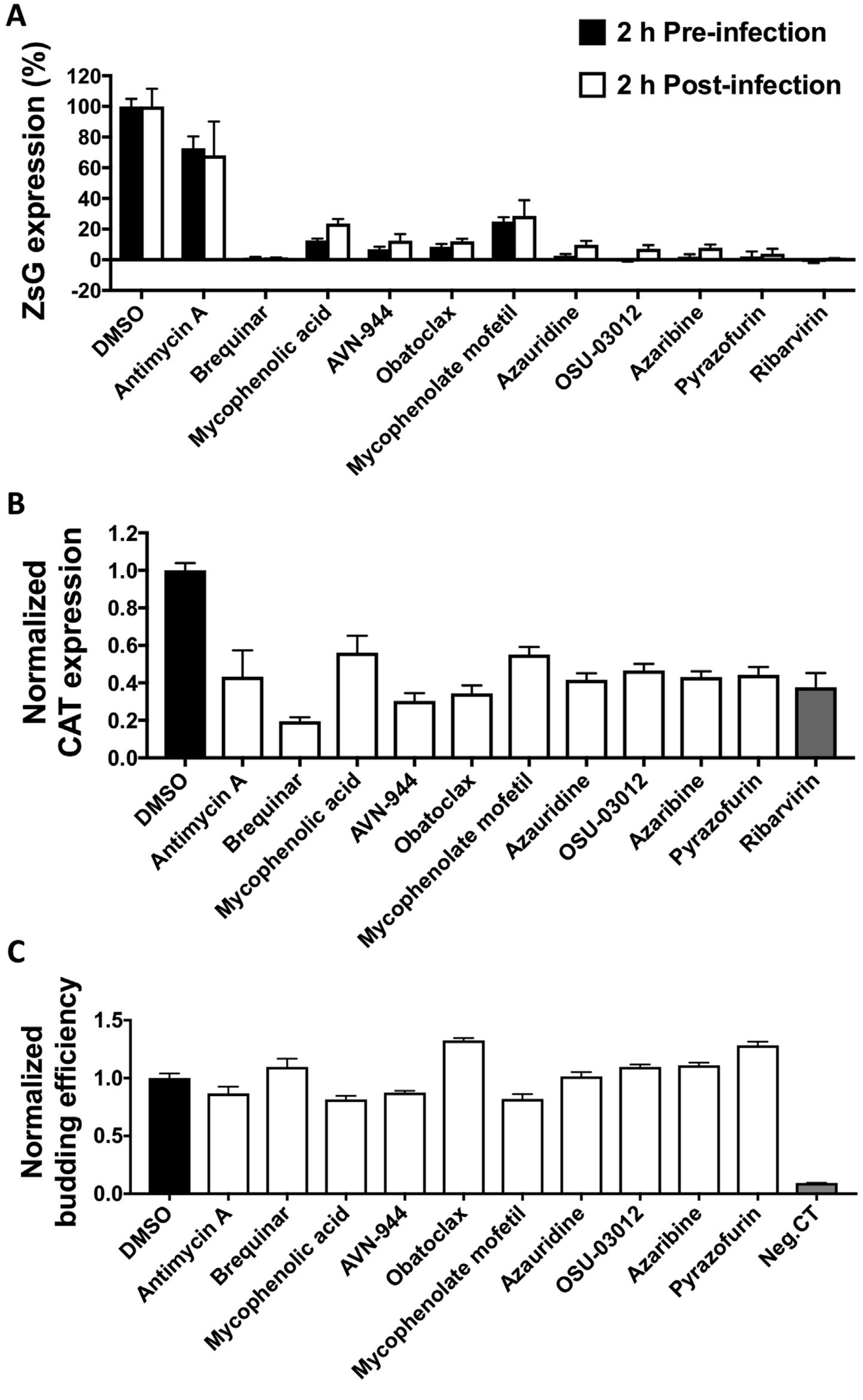

Fig. 3. Effect of selected hits on different steps of LCMV multiplication. (A) Compound effects on LCMV cell entry. A549 cells were treated with the indicated compounds (5 μM) starting 2 h prior to or after infection (MOI = 0.5) with the single cycle infectious rLCMV/ΔGPC/ZsG pseudotyped with GPC. At 48 h pi, cells were fixed, and infected cells were identified based on ZsG expression. ZsG expression was normalized to VC- treated samples. (B) Compound effects on LCMV minigenome (MG)-derived reporter gene expression. 293T cells were transfected with plasmids expressing cytomegalovirus T7 polymerase promoter (pC-T7), pMG-chloramphenicol acetyl transferase (CAT), pC-NP (NP), and pC-L polymerase. At 5 h post-transfection, fresh media containing each selected hit were added, and cells were incubated for 48 h. CAT expression was determined by CAT-enzyme-linked immunosorbent assay (ELISA). Optical density values were normalized to values obtained with VC-treated control cells. (C) Effects of compounds on Z matrix protein budding activity. 293T cells were transfected with pC-LASV-Z-Gaussia luciferase (GLuc) and treated (5 μM) with selected hits. At 48 h post-treatment, we determined GLuc activity in tissue culture supernatants (TCS) and whole cell lysates (WCL). Levels of GLuc in TCS and WCL were used as surrogates of Z expression levels. Budding efficiency was defined as the ratio $Z_{VLP}/Z_{VLP} + Z_{WCL}$. We used mutant Z-G2A-GLuc as negative control. Budding efficiency results were normalized to VC (DMSO)-treated group, which was adjusted to 1.

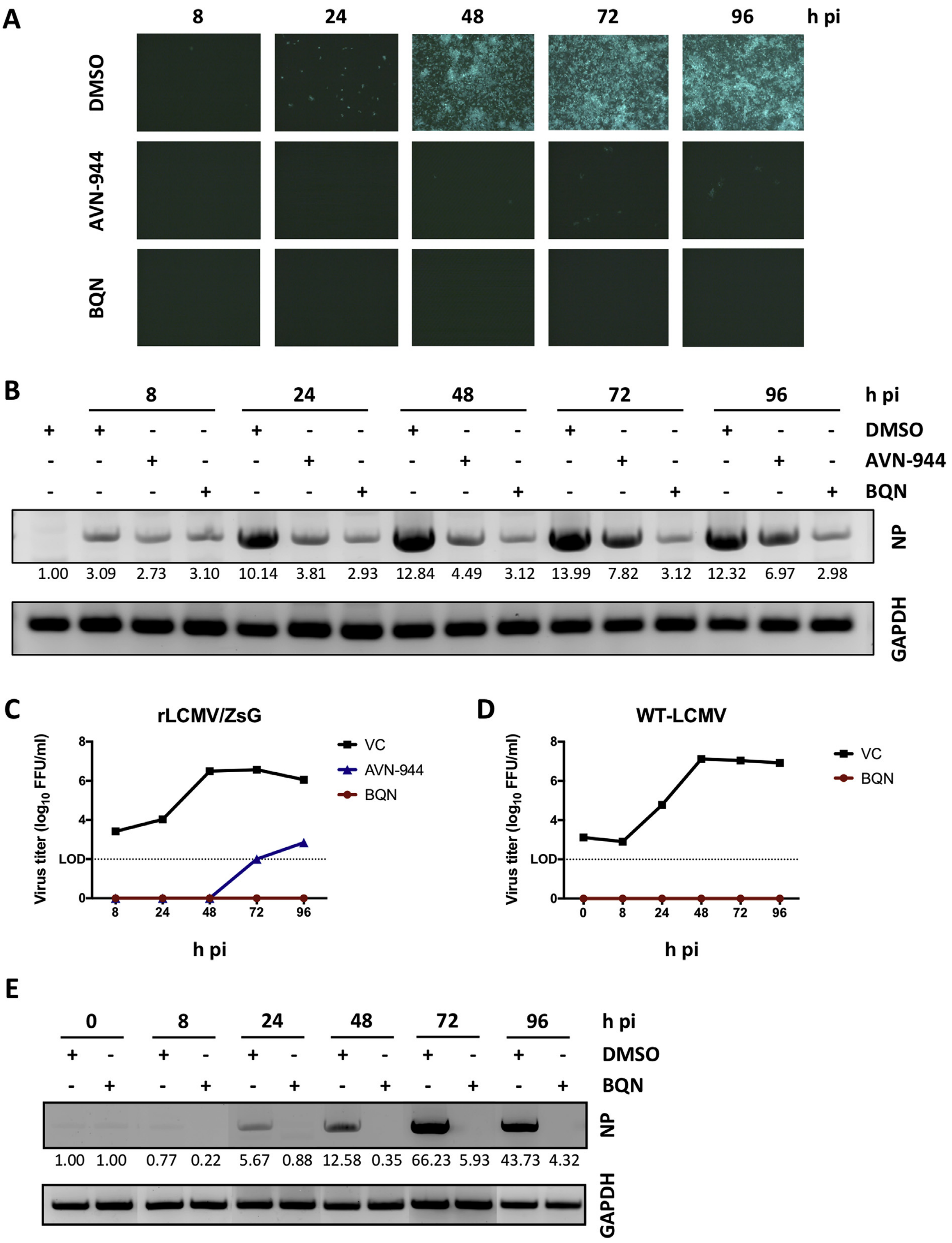

(caption on next page)

expression. All five compounds strongly inhibited rLASV/GFP and r3Can/GFP multiplication in IFN-deficient Vero E6 cells (Emonet et al., 2011) (Fig. 6B). AVN-944, BQN, MPA, OLX, and PYF exhibited also a potent inhibitory effect on production of infectious wild-type LASV (Fig. 6C) that correlated with inhibition of cell-to-cell propagation of LASV as illustrated for BQN (Fig. 6D).

3.7. Myeloid cell leukemia (MCL1), the target of OLX, is required for normal LCMV multiplication

The validated MCL1 inhibitor OLX (Nguyen et al., 2015) had potent anti-LCMV activity. Consistent with this finding, ML311, another validated inhibitor of MCL1 (Bannister et al., 2010), also exhibited robust

Fig. 4. Effect of selected hits on virus propagation, viral RNA synthesis, and production of infectious progeny. (A) A549 cells were infected (MOI = 0.01) with rLCMV/ZsG-P2A-NP and treated (5 μM) with AVN-944 or BQN. At the indicated h pi, tissue culture supernatants (TCS) were collected, FluoroBrite-DMEM added to cells and representative images of ZsG expression were obtained using live cell fluorescent microscopy. (B) After image collection, whole cell lysates (WCL) from rLCMV/ZsG-infected cells were prepared and total cellular RNA isolated. Equal amounts (2 μg) of RNA from each sample were analyzed by semi-quantitative reverse transcriptase-polymerase chain reaction with specific primers to assess levels of viral RNA synthesis of NP and the housekeeping gene GAPDH. Numbers below the panel showing RT-PCR products generated using NP-specific primers correspond to densitometry quantification of each band normalized to GAPDH. Virus titers of rLCMV/ZsG (C) and WT-LCMV (D) in TCS were determined by focus forming assay. Results for virus titers represent means ± standard deviation (SD) of two independent experiments. Each independent experiment consisted of three replicates. Titers obtained at 0 h pi were in all cases less than the limit of detection. VC corresponds to vehicle-treated cells. Dotted line indicates the limit of detection (LOD). (E) At the indicated h pi, total cellular RNA was isolated and viral RNA levels were detected by semi-quantitative RT-PCR using NP-specific primers. Levels of GAPDH mRNA were determined by semi-quantitative RT-PCR using GAPDH-specific primers. Each number indicates the band density normalized to GAPDH. Numbers below the panel showing RT-PCR products generated using NP-specific primers correspond to densitometry quantification of each band normalized to GAPDH.

anti-LCMV activity (Fig. 7A), further supporting the antiviral effect of MCL1 inhibition. Accordingly, multiplication of rLCMV/ZsG was significantly reduced in MCL1 knockout MEF (Fig. 7B). These findings suggest a potential pro-viral role of MCL1 in the replication cycle of LCMV.

4. Discussion

The mammarenavirus replication cycle involves a complex network of protein-protein interactions, including the participation of both viral and host cell proteins. Thus, a large number of host cell factors participate in cell entry of arenavirions (Iwasaki et al., 2014; Jae and Brummelkamp, 2015; Jae et al., 2014; Oppliger et al., 2016; Panda et al., 2011) that ultimately results in the release of the vRNP into the cytoplasm. Similarly, formation of a functional vRNP requires interactions between viral proteins but also between viral and host cell proteins (Ahlquist et al., 2003; Bortz et al., 2011). Likewise, as with other bona fide viral budding proteins (Wolff et al., 2013), the mammarenavirus Z matrix protein interacts with different components of the multivesicular body pathway of the infected cell to direct mammarenavirus budding.

Direct-acting antivirals (DAAs) that target specific viral gene products and functions are likely to be well tolerated by the infected host, but commonly, drug resistant variants emerge (Domingo et al., 2006). Combination therapy has proven effective to reduce and delay the selection of escape mutants. Such combinations do not entirely solve this problem, as illustrated by the selection of hepatitis C virus-resistant variants in patients who fail to control the virus during asunaprevir and daclatasvir treatment (Kai et al., 2017). On the other hand, the emergence of viral variants resistant to host-targeting antivirals (HTAs) is usually significantly reduced or entirely absent. Intra-host virus evolution is unlikely to result in viral variants able to escape from

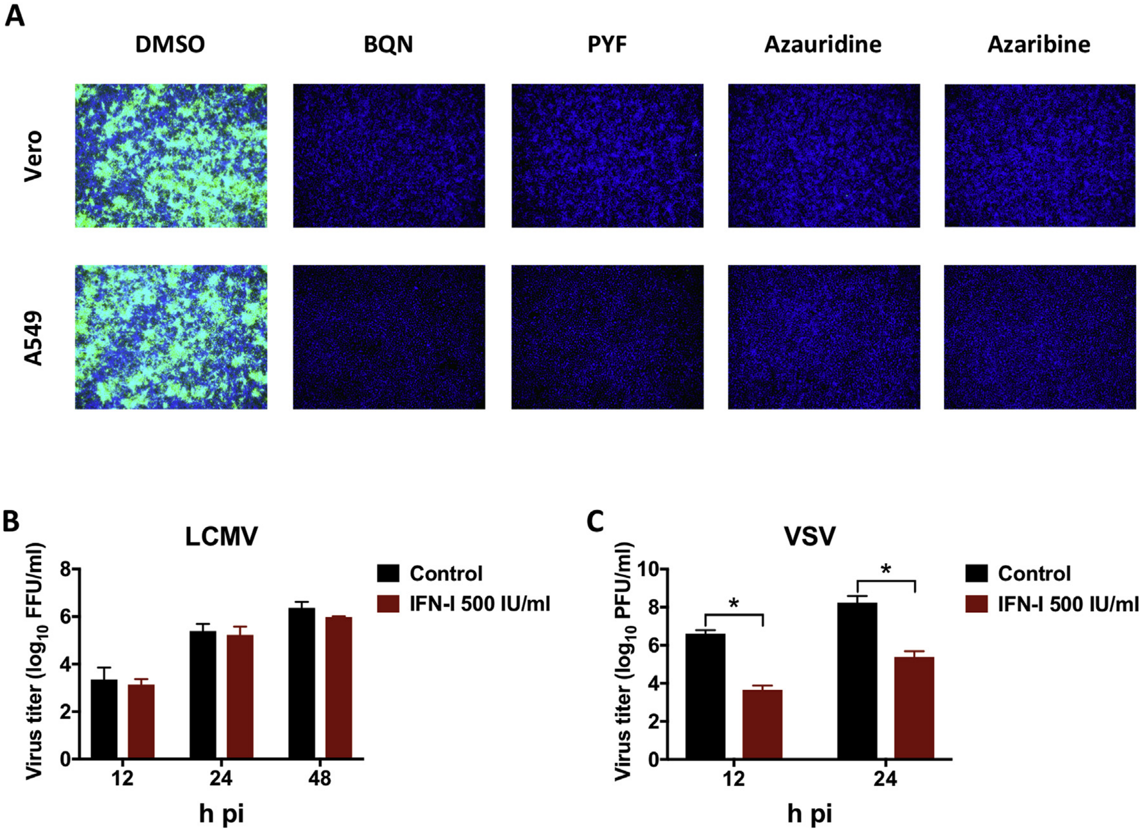

Fig. 5. Interferon-stimulated genes do not contribute to the antiviral activity of selected representative hits. (A) Vero (interferon type 1 (IFN-I)-deficient) and A549 (IFN-I-competent) cells were infected with rLCMV/ZsG at MOI of 0.01 (A549 cells) or 0.001 (Vero cells) in the presence of BQN, PYF, azauridine, azaribine (5 μM), or VC. At 48 h pi, cells were fixed with 4% PFA, and infected cells were identified based on ZsG expression. Nuclei were stained with 4′,6-diamidino-2-phenylindole. Vero cells were treated with 500 IU/ml of IFN-I for 16 h and then infected with LCMV (MOI = 0.01) (B) or VSIV (MOI = 0.1) (C). At the indicated h pi, tissue culture supernatants were collected, and titers of infectious virus were determined. IFN-I was maintained throughout the infection. Statistical significance was calculated by multiple *t*-test. *$p < 0.05$ as indicated among the groups.

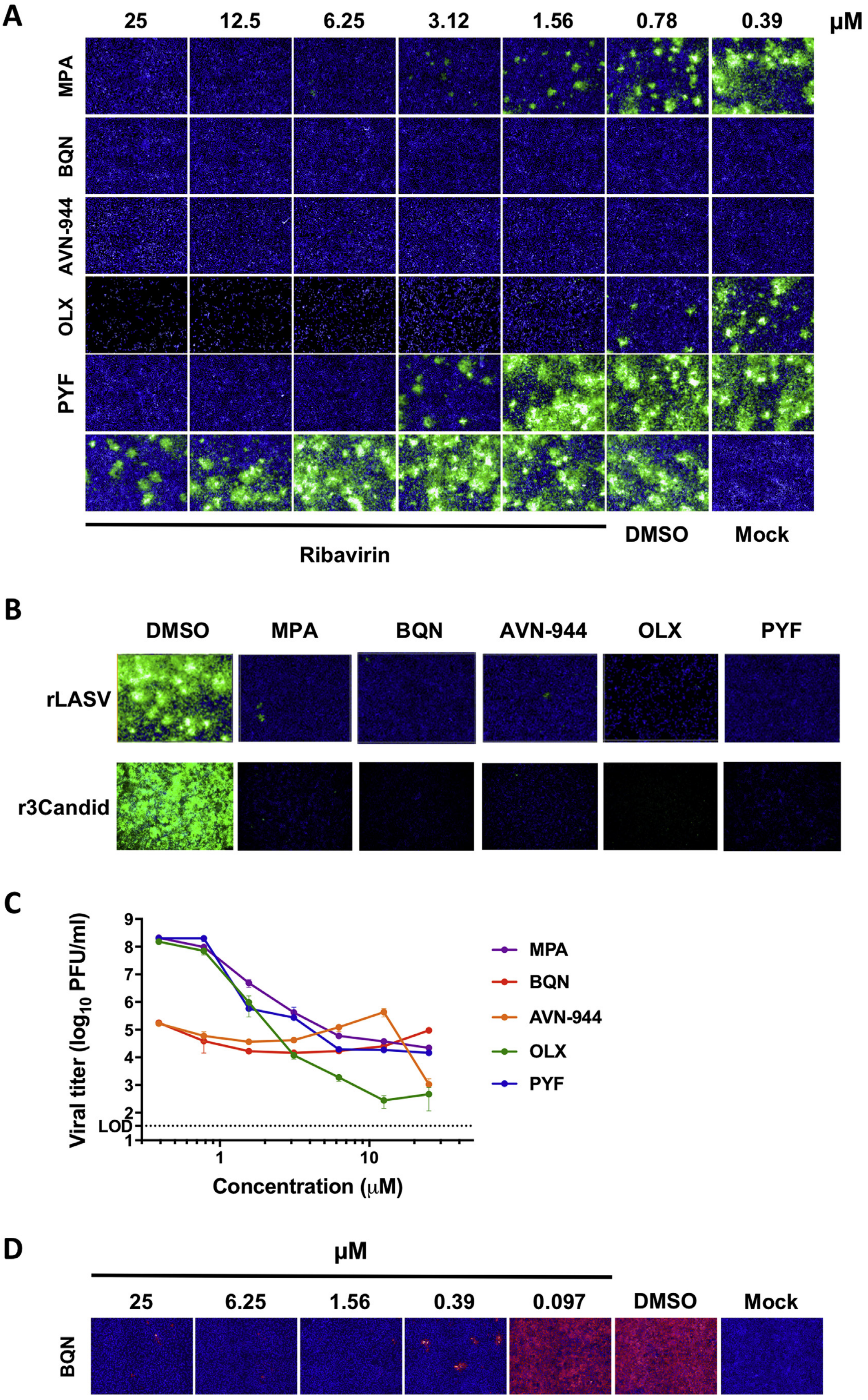

(caption on next page)

Fig. 6. Inhibitory effect of selected compounds on Lassa virus (LASV) and Junín virus (JUNV) multiplication. (A) A549 cells were infected (MOI = 0.1) with recombinant LASV expressing green fluorescent protein (rLASV/GFP) in the presence of the indicated compounds and concentrations and controls, including ribavirin (positive control), dimethyl sulfoxide (vehicle control), and mock infection. At 48 h pi, cells were fixed (4% paraformaldehyde), and Hoechst 33342 dye was used to stain cell nuclei. Green fluorescent protein (GFP) expression was detected using the Operetta High-Content Imaging. (B) Vero cells were infected (MOI = 0.1) with rLASV/GFP or tri-segmented form of the live attenuated vaccine strain Candid#1 of JUNV expressing green fluorescent protein (r3Can/GFP) in the presence of indicated compounds (5 μM). At 48 (rLASV/GFP) or 96 (r3Can/GFP) h pi, cells were fixed and stained with either Hoechst 33342 dye (rLASV/GFP-infected cells) or DAPI (r3Can/GFP-infected cells). Virus multiplication was assessed based on GFP expression. (C) A549 cells were infected (MOI = 0.1) with LASV in the presence of increasing concentrations of the indicated compounds. At 48 h pi, tissue culture supernatants were collected and virus titers were determined by plaque assay. The dotted line indicates the limit of detection (LOD). (D) A549 cells were infected with LASV (MOI = 0.1) and treated with the indicated concentrations of BQN. At 48 h pi, expression infected cells were identified by immunofluorescence using a mouse monoclonal antibody to LASV NP, followed by a secondary anti-mouse Alexa Fluor 594-conjugated antibody.

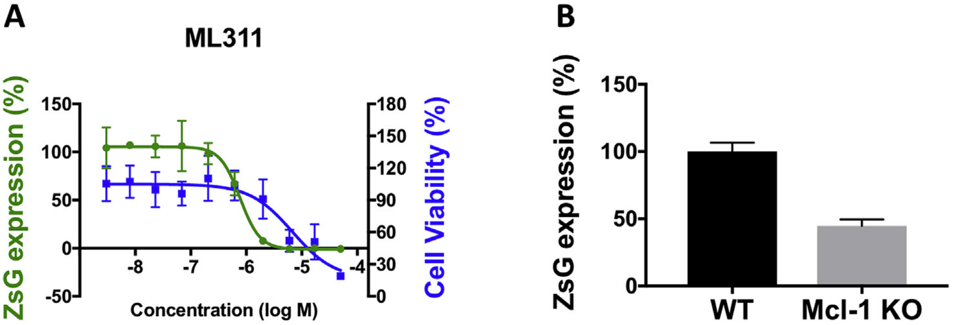

Fig. 7. MCL1 is required for optimal levels of LCMV multiplication. (A) Determination of EC_{50} and CC_{50} of the MCL1 inhibitor ML311. To determine the ML311 EC_{50}, A549 cells were treated with serial dilutions of ML311 starting 2 h prior infection (MOI = 0.01) with rLCMV/ZsG. At 48 h pi, ZsG expression was measured. To determine the ML311 CC_{50}, cells were treated with serial dilutions of the compound, and 48 h later cell viability was determined using the CellTiter 96 AQueous One Solution reagent. Data were normalized to VC-treated control group that was adjusted to 100%. (B). MCL1 knock-out mouse embryonic fibroblasts (MEF/MCL1-KO) and MEF/MCL1-KO reconstituted with a lentivirus expressing MCL1 (MEF/MCL1) were infected with rLCMV/ZsG (MOI = 0.01). At 48 h pi, virus multiplication was assessed based on ZsG expression.

inhibitors that disrupt cellular functions required for the completion of steps of the virus live cycle. In this regard, drug repurposing screens have become instrumental in identifying known drugs that exhibit the previously unknown ability of disrupting virus-host cell protein interactions required throughout the virus replication cycle.

Several distinct classes of compounds inhibit mammarenavirus glycoprotein precursor (GPC)-mediated membrane fusion by binding to a common site on GPC and stabilizing the pre-fusion GPC complex (Bolken et al., 2006; Larson et al., 2008; Lee et al., 2008; Rathbun et al., 2015; York et al., 2008). In contrast, the top-ranked hits with anti-LCMV activity that we identified within the ReFRAME library had minimal effects on virion cell entry, but rather they exerted their anti-LCMV activity by interfering with the activity of the vRNP. Notably, several of these hits had, under our experimental conditions, lower EC_{50} values than that determined for favipiravir, a broad-spectrum antiviral that protects against disease in domesticated guinea pigs (*Cavia porcellus*) infected with JUNV (Gowen et al., 2013) or LASV (Safronetz et al., 2015).

Seven of the ten top hits we identified in our screen of compounds with anti-LCMV activity target the host cell machinery of nucleotide synthesis. MPA, AVN-944, and mycophenolate mofetil are IMPDH inhibitors that block *de novo* biosynthesis of purine nucleotides (Floryk and Thompson, 2008; Ishitsuka et al., 2005; Nakanishi et al., 2010; Sintchak et al., 1996). BQN is a known inhibitor of DHODH (Sykes et al., 2016), whereas PYF, azauridine, and azaribine inhibit the activity of UMPS (Meza-Avina et al., 2010). Both DHODH and UMPS are key enzymes on the cellular pathway *of de novo* pyrimidine synthesis (Meza-Avina et al., 2010; Sykes et al., 2016). Notably, DHODH and IMPDH inhibitors also have antiviral activity against LASV and JUNV. Related viruses are likely to rely on the same host machinery, suggesting that inhibitors of these enzymes could be developed into broad-spectrum anti-mammarenavirus therapeutics. Previous studies have documented the antiviral activity of MPA (Madrid et al., 2013) and azauridine (Welch et al., 2016) against LASV. Likewise, the anti-LASV activity of the kinase inhibitor OSU-03012 we identified in the ReFRAME library had been previously documented in a screen of inhibitors of cellular kinases for compounds with broad-spectrum antiviral activity against certain hemorrhagic fever-causing viruses (Mohr et al., 2015). These findings further validate the ReFRAME library as a valuable drug repurposing library.

Inhibition of pyrimidine biosynthesis has been proposed to suppress viral growth by enhancing the type I interferon (IFN-I)-mediated innate immunity responses in infected cells (Lucas-Hourani et al., 2013). However, we observed that pyrimidine biosynthesis inhibitors BQN, PYF, azauridine, and azaribine exerted similar anti-LCMV activity in both IFN-I-deficient (Vero E6) and IFN-I-competent (A549) cells (Fig. 5), suggesting IFN-I-independent anti-LCMV activity. Previously, pyrimidine biosynthesis inhibition by a tetrahydrobenzothiazole compound with broad spectrum antiviral activity was associated with induction of an IFN-I-independent antiviral state as determined by expression of a variety of IFN-stimulated genes (ISGs) (Chung et al., 2016). Moreover, compound SW835, a racemic version of a DHODH inhibitor (GSK983) that has broad spectrum antiviral activity, inhibited replication of Ebola virus, VSIV, and Zika virus in cultured cells. This inhibition was associated with induced expression of ISGs that occurred in the absence of IFN-I production but required interferon regulatory transcription factor, IRF1, and the DNA damage response serine/threonine kinase ATM (Luthra et al., 2018).

These findings raise the possibility that the anti-LCMV activity of DHODH inhibitors we observed in Vero E6 cells was mediated by an IFN-I independent induction of ISGs. However, treatment of Vero E6 cells with exogenous IFN-I resulted in a strong inhibition of VSIV multiplication, whereas LCMV multiplication was minimally affected. This finding is consistent with the known resistance of LCMV, LASV, and JUNV to the IFN-I induced cell antiviral state. Despite the potent antiviral activity of pyrimidine biosynthesis inhibitors in cell-based infection assays, the development of these inhibitors as antiviral drugs may be prevented by high blood uridine concentrations that facilitate a salvage pathway for synthesis of pyrimidine nucleotides (Wang et al., 2011). However, it should be noted that the DHODH inhibitor teriflunomide is efficient in the treatment of multiple sclerosis (MS) patients (Aly et al., 2017). The proposed primary mechanism of action of teriflunomide against MS is via its effects on proliferation of activated lymphocytes with a high pyrimidine demand that cannot be met through the salvage pathway (Bar-Or, 2014). It is plausible that rapidly multiplying viruses, like LASV, have pyrimidine requirements that are not efficiently provided by the salvage pathway, which could result in reduced viral load that could provide the infected host with a window of opportunity to mount an effective immune response to control and eliminate the infection.

MCL1, an antiapoptotic member of the BCL2 protein family and key regulator of mitochondrial homeostasis, plays a pivotal role in cell survival and homeostasis by counteracting the activity of pro-apoptotic members of the BCL2 family. Upregulation of MCL1 occurs in various types of human cancer (Xiang et al., 2018), and downregulation of MCL1 increases the sensitivity of tumor cells to various anticancer drugs (Lestini et al., 2009; Osaki et al., 2016). The BCL2 homology domain 3 (BH3) mimetic, OLX, antagonizes MCL1 and inhibits all anti-apoptotic proteins of the BCL2 family (Nguyen et al., 2007).

The mechanisms by which OLX interferes with mammarenavirus multiplication remain to be elucidated. OLX induces defective autophagy and mitochondrial stress (Sulkshane and Teni, 2017), which could result in a cellular environment that restricts mammarenavirus multiplication. In addition, OLX inhibits cell entry of influenza A virus (Denisova et al., 2012) and several alpha-and flaviviruses (Varghese et al., 2017) by inhibiting endosomal acidification that prevents pH-dependent fusion required for entry of particles of these viruses. Intriguingly, cell entry of mammarenaviruses, including LCMV and LASV, also requires an acidic environment of late endosomes for pH-dependent fusion between viral and cell membranes (Eschli et al., 2006; Kunz et al., 2002). However, we found that addition of OLX at 2 h pi, a time at which LCMV cell entry processed has been completed (Rojek et al., 2008), resulted in inhibition of LCMV replication and gene expression, suggesting that mammarenavirion cell entry is not targeted by OLX. Interestingly, the susceptibility of chronic lymphocytic leukemia (CLL) cells to the oncolytic activity of VSIV was enhanced by treatment with OLX (Samuel et al., 2010), despite the same acidic requirement of VSIV for cell entry (Regan and Whittaker, 2013).

Our screen also identified antimycin A as a compound with anti-LCMV activity. Antimycin A targets the mitochondrial respiratory complex III (Labs et al., 2016), leading to increased generation of reactive oxygen species (ROS) and ATP synthase inhibition (Georgakopoulos et al., 2017). This impairment of cellular mitochondrial respiration can promote induction of antiviral innate immune responses affecting virus multiplication (Kim et al., 2013) and lead to suppression of *de novo* pyrimidine biosynthesis with antiviral manifestations (Raveh et al., 2013).

5. Conclusion

Screening of the ReFRAME library for inhibitors of LCMV multiplication identified ten compounds with potent dose-dependent anti-LCMV activity. Seven of the hits targeted enzymes involved in purine (IMPDH) and pyrimidine (DHODH and UMPS) nucleotides biosynthesis. In addition, inhibitors of the pro-viral MCL1 protein and the mitochondrial respiratory complex III exhibited also strong anti-LCMV activity. Inhibitors of IMPDH, DHODH, UMPS, and MCL1 also had strong inhibitory activity against JUNV and LASV.

Acknowledgments

We thank Laura Bollinger (IRF-Frederick) for editing the manuscript. This work was funded in part through Battelle Memorial Institute's prime contract with the US National Institute of Allergy and Infectious Diseases (NIAID) under Contract No. HHSN272200700016I (Y.C., J.H.K.) and NIH/NIAID grants AI125626 and AI128556 (JCT). This is manuscript # 29829 from The Scripps Research Institute. The content of this publication does not necessarily reflect the views or policies of the US Department of Health and Human Services, or the institutions and companies affiliated with the authors.

Appendix A. Supplementary data

Supplementary data to this article can be found online at https://doi.org/10.1016/j.antiviral.2019.104558.

References

Ahlquist, P., Noueiry, A.O., Lee, W.M., Kushner, D.B., Dye, B.T., 2003. Host factors in positive-strand RNA virus genome replication. J. Virol. 77, 8181–8186.

Aly, L., Hemmer, B., Korn, T., 2017. From leflunomide to teriflunomide: drug development and immunosuppressive oral drugs in the treatment of multiple sclerosis. Curr. Neuropharmacol. 15, 874–891.

Ashburn, T.T., Thor, K.B., 2004. Drug repositioning: identifying and developing new uses for existing drugs. Nat. Rev. Drug Discov. 3, 673–683.

Bannister, T., Koenig, M., He, Y., Mishra, J., Spicer, T., Minond, D., Saldanha, A., Mercer, B.A., Cameron, M., Lena, R., Carlson, N., Richard, D., Cardone, M., Hodder, P., 2010. ML311: A Small Molecule that Potently and Selectively Disrupts the Protein-Protein Interaction of Mcl-1 and Bim: A Probe for Studying Lymphoid Tumorigenesis, Probe Reports from the NIH Molecular Libraries Program, Bethesda (MD).

Bar-Or, A., 2014. Teriflunomide (Aubagio(R)) for the treatment of multiple sclerosis. Exp. Neurol. 262, 57–65.

Barton, L.L., Mets, M.B., Beauchamp, C.L., 2002. Lymphocytic choriomeningitis virus: emerging fetal teratogen. Am. J. Obstet. Gynecol. 187, 1715–1716.

Battegay, M., 1993. [Quantification of lymphocytic choriomeningitis virus with an immunological focus assay in 24 well plates]. ALTEX 10, 6–14.

Bolken, T.C., Laquerre, S., Zhang, Y., Bailey, T.R., Pevear, D.C., Kickner, S.S., Sperzel, L.E., Jones, K.F., Warren, T.K., Amanda Lund, S., Kirkwood-Watts, D.L., King, D.S., Shurtleff, A.C., Guttieri, M.C., Deng, Y., Bleam, M., Hruby, D.E., 2006. Identification and characterization of potent small molecule inhibitor of hemorrhagic fever New World arenaviruses. Antivir. Res. 69, 86–97.

Borio, L., Inglesby, T., Peters, C.J., Schmaljohn, A.L., Hughes, J.M., Jahrling, P.B., Ksiazek, T., Johnson, K.M., Meyerhoff, A., O'Toole, T., Ascher, M.S., Bartlett, J., Breman, J.G., Eitzen Jr., E.M., Hamburg, M., Hauer, J., Henderson, D.A., Johnson, R.T., Kwik, G., Layton, M., Lillibridge, S., Nabel, G.J., Osterholm, M.T., Perl, T.M., Russell, P., Tonat, K., Working Group on Civilian, B., 2002. Hemorrhagic fever viruses as biological weapons: medical and public health management. JAMA 287, 2391–2405.

Bortz, E., Westera, L., Maamary, J., Steel, J., Albrecht, R.A., Manicassamy, B., Chase, G., Martinez-Sobrido, L., Schwemmle, M., Garcia-Sastre, A., 2011. Host- and strain-specific regulation of influenza virus polymerase activity by interacting cellular proteins. mBio 2.

Buchmeier, M.J., Peters, C.J., de la Torre, J.C., 2007. Arenaviridae: the viruses and their replication. In: Knipe, D.M., Holey, P.M. (Eds.), Field's Virology, 5 ed. Lippincott Williams & Wilkins, Philadelphia, PA, pp. 1791–1851.

Cai, Y., Iwasaki, M., Beitzel, B.F., Yu, S., Postnikova, E.N., Cubitt, B., DeWald, L.E., Radoshitzky, S.R., Bollinger, L., Jahrling, P.B., Palacios, G.F., de la Torre, J.C., Kuhn, J.H., 2018. Recombinant Lassa Virus Expressing Green Fluorescent Protein as a Tool for High-Throughput Drug Screens and Neutralizing Antibody Assays. Viruses 10.

Capul, A.A., de la Torre, J.C., 2008. A cell-based luciferase assay amenable to high-throughput screening of inhibitors of arenavirus budding. Virology 382, 107–114.

Cashman, K.A., Smith, M.A., Twenhafel, N.A., Larson, R.A., Jones, K.F., Allen 3rd, R.D., Dai, D., Chinsangaram, J., Bolken, T.C., Hruby, D.E., Amberg, S.M., Hensley, L.E., Guttieri, M.C., 2011. Evaluation of Lassa antiviral compound ST-193 in a Guinea pig model. Antivir. Res. 90, 70–79.

Chung, D.H., Golden, J.E., Adcock, R.S., Schroeder, C.E., Chu, Y.K., Sotsky, J.B., Cramer, D.E., Chilton, P.M., Song, C., Anantpadma, M., Davey, R.A., Prodhan, A.I., Yin, X., Zhang, X., 2016. Discovery of a broad-spectrum antiviral compound that inhibits pyrimidine biosynthesis and establishes a type 1 interferon-independent antiviral state. Antimicrob. Agents Chemother. 60, 4552–4562.

Damonte, E.B., Coto, C.E., 2002. Treatment of arenavirus infections: from basic studies to the challenge of antiviral therapy. Adv. Virus Res. 58, 125–155.

Denisova, O.V., Kakkola, L., Feng, L., Stenman, J., Nagaraj, A., Lampe, J., Yadav, B., Aittokallio, T., Kaukinen, P., Ahola, T., Kuivanen, S., Vapalahti, O., Kantele, A., Tynell, J., Julkunen, I., Kallio-Kokko, H., Paavilainen, H., Hukkanen, V., Elliott, R.M., De Brabander, J.K., Saelens, X., Kainov, D.E., 2012. Obatoclax, saliphenylhalamide, and gemcitabine inhibit influenza a virus infection. J. Biol. Chem. 287, 35324–35332.

Domingo, E., Martin, V., Perales, C., Grande-Perez, A., Garcia-Arriaza, J., Arias, A., 2006. Viruses as quasispecies: biological implications. Curr. Top. Microbiol. Immunol. 299, 51–82.

Emonet, S.F., Garidou, L., McGavern, D.B., de la Torre, J.C., 2009. Generation of recombinant lymphocytic choriomeningitis viruses with trisegmented genomes stably expressing two additional genes of interest. Proc. Natl. Acad. Sci. U. S. A. 106, 3473–3478.

Emonet, S.F., Seregin, A.V., Yun, N.E., Poussard, A.L., Walker, A.G., de la Torre, J.C., Paessler, S., 2011. Rescue from cloned cDNAs and in vivo characterization of recombinant pathogenic Romero and live-attenuated Candid #1 strains of Junin virus, the causative agent of Argentine hemorrhagic fever disease. J. Virol. 85, 1473–1483.

Enria, D.A., Briggiler, A.M., Sanchez, Z., 2008. Treatment of Argentine hemorrhagic fever. Antivir. Res. 78, 132–139.

Eschli, B., Quirin, K., Wepf, A., Weber, J., Zinkernagel, R., Hengartner, H., 2006. Identification of an N-terminal trimeric coiled-coil core within arenavirus glycoprotein 2 permits assignment to class I viral fusion proteins. J. Virol. 80, 5897–5907.

Fischer, S.A., Graham, M.B., Kuehnert, M.J., Kotton, C.N., Srinivasan, A., Marty, F.M., Comer, J.A., Guarner, J., Paddock, C.D., DeMeo, D.L., Shieh, W.J., Erickson, B.R., Bandy, U., DeMaria Jr., A., Davis, J.P., Delmonico, F.L., Pavlin, B., Likos, A., Vincent, M.J., Sealy, T.K., Goldsmith, C.S., Jernigan, D.B., Rollin, P.E., Packard, M.M., Patel, M., Rowland, C., Helfand, R.F., Nichol, S.T., Fishman, J.A., Ksiazek, T., Zaki, S.R., Team, L.i.T.R.I., 2006. Transmission of lymphocytic choriomeningitis virus by organ transplantation. N. Engl. J. Med. 354, 2235–2249.

Floryk, D., Thompson, T.C., 2008. Antiproliferative effects of AVN944, a novel inosine 5-monophosphate dehydrogenase inhibitor, in prostate cancer cells. Int. J. Cancer 123, 2294–2302.

Freedman, D.O., Woodall, J., 1999. Emerging infectious diseases and risk to the traveler. Med. Clin. N. Am. 83, 865–883 (v).

Geisbert, T.W., Jahrling, P.B., 2004. Exotic emerging viral diseases: progress and challenges. Nat. Med. 10, S110–S121.

Georgakopoulos, N.D., Wells, G., Campanella, M., 2017. The pharmacological regulation of cellular mitophagy. Nat. Chem. Biol. 13, 136–146.

Giachetti, C., Holland, J.J., 1989. Vesicular stomatitis virus and its defective interfering particles exhibit in vitro transcriptional and replicative competition for purified L-NS polymerase molecules. Virology 170, 264–267.

Gowen, B.B., Juelich, T.L., Sefing, E.J., Brasel, T., Smith, J.K., Zhang, L., Tigabu, B., Hill, T.E., Yun, T., Pietzsch, C., Furuta, Y., Freiberg, A.N., 2013. Favipiravir (T-705) inhibits Junin virus infection and reduces mortality in a Guinea pig model of Argentine hemorrhagic fever. PLoS Neglected Trop. Dis. 7, e2614.

Gunther, S., Lenz, O., 2004. Lassa virus. Crit. Rev. Clin. Lab. Sci. 41, 339–390.

Isaacson, M., 2001. Viral hemorrhagic fever hazards for travelers in Africa. Clin. Infect. Dis.: Off. Publ. Infect. Dis. Soc. Am. 33, 1707–1712.

Ishitsuka, K., Hideshima, T., Hamasaki, M., Raje, N., Kumar, S., Podar, K., Le Gouill, S., Shiraishi, N., Yasui, H., Roccaro, A.M., Tai, Y.Z., Chauhan, D., Fram, R., Tamura, K., Jain, J., Anderson, K.C., 2005. Novel inosine monophosphate dehydrogenase inhibitor VX-944 induces apoptosis in multiple myeloma cells primarily via caspase-independent AIF/Endo G pathway. Oncogene 24, 5888–5896.

Iwasaki, M., de la Torre, J.C., 2018. A highly conserved leucine in mammarenavirus matrix Z protein is required for Z interaction with the virus L polymerase and Z stability in cells harboring an active viral ribonucleoprotein. J. Virol. 92.

Iwasaki, M., Minder, P., Cai, Y., Kuhn, J.H., Yates 3rd, J.R., Torbett, B.E., de la Torre, J.C., 2018. Interactome analysis of the lymphocytic choriomeningitis virus nucleoprotein in infected cells reveals ATPase Na + /K + transporting subunit Alpha 1 and prohibitin as host-cell factors involved in the life cycle of mammarenaviruses. PLoS Pathog. 14, e1006892.

Iwasaki, M., Ngo, N., de la Torre, J.C., 2014. Sodium hydrogen exchangers contribute to arenavirus cell entry. J. Virol. 88, 643–654.

Jae, L.T., Brummelkamp, T.R., 2015. Emerging intracellular receptors for hemorrhagic fever viruses. Trends Microbiol. 23, 392–400.

Jae, L.T., Raaben, M., Herbert, A.S., Kuehne, A.I., Wirchnianski, A.S., Soh, T.K., Stubbs, S.H., Janssen, H., Damme, M., Saftig, P., Whelan, S.P., Dye, J.M., Brummelkamp, T.R., 2014. Virus entry. Lassa virus entry requires a trigger-induced receptor switch. Science 344, 1506–1510.

Jahrling, P.B., Keith, L., St Claire, M., Johnson, R.F., Bollinger, L., Lackemeyer, M.G., Hensley, L.E., Kindrachuk, J., Kuhn, J.H., 2014. The NIAID Integrated Research Facility at Frederick, Maryland: a unique international resource to facilitate medical countermeasure development for BSL-4 pathogens. Pathog Dis 71, 213–219.

Jahrling, P.B., Peters, C.J., 1992. Lymphocytic choriomeningitis virus. A neglected pathogen of man. Arch. Pathol. Lab Med. 116, 486–488.

Janes, J., Young, M.E., Chen, E., Rogers, N.H., Burgstaller-Muehlbacher, S., Hughes, L.D., Love, M.S., Hull, M.V., Kuhen, K.L., Woods, A.K., Joseph, S.B., Petrassi, H.M., McNamara, C.W., Tremblay, M.S., Su, A.I., Schultz, P.G., Chatterjee, A.K., 2018. The ReFRAME library as a comprehensive drug repurposing library and its application to the treatment of cryptosporidiosis. Proc. Natl. Acad. Sci. U. S. A. 115, 10750–10755.

Janosko, K., Holbrook, M.R., Adams, R., Barr, J., Bollinger, L., Newton, J.T., Ntiforo, C., Coe, L., Wada, J., Pusl, D., Jahrling, P.B., Kuhn, J.H., Lackemeyer, M.G., 2016. Safety precautions and operating procedures in an (A)BSL-4 laboratory: 1. Biosafety level 4 suit laboratory suite entry and exit procedures. J. Vis. Exp.(116). https://doi.org/10.3791/52317.

Kai, Y., Hikita, H., Morishita, N., Murai, K., Nakabori, T., Iio, S., Hagiwara, H., Imai, Y., Tamura, S., Tsutsui, S., Naito, M., Nishiuchi, M., Kondo, Y., Kato, T., Suemizu, H., Yamada, R., Oze, T., Yakushijin, T., Hiramatsu, N., Sakamori, R., Tatsumi, T., Takehara, T., 2017. Baseline quasispecies selection and novel mutations contribute to emerging resistance-associated substitutions in hepatitis C virus after direct-acting antiviral treatment. Sci. Rep. 7, 41660.

Kim, H.J., Kim, C.H., Ryu, J.H., Kim, M.J., Park, C.Y., Lee, J.M., Holtzman, M.J., Yoon, J.H., 2013. Reactive oxygen species induce antiviral innate immune response through IFN-lambda regulation in human nasal epithelial cells. Am. J. Respir. Cell Mol. Biol. 49, 855–865.

Kunz, S., Borrow, P., Oldstone, M.B., 2002. Receptor structure, binding, and cell entry of arenaviruses. Curr. Top. Microbiol. Immunol. 262, 111–137.

Labs, M., Ruhle, T., Leister, D., 2016. The antimycin A-sensitive pathway of cyclic electron flow: from 1963 to 2015. Photosynth. Res. 129, 231–238.

Larson, R.A., Dai, D., Hosack, V.T., Tan, Y., Bolken, T.C., Hruby, D.E., Amberg, S.M., 2008. Identification of a broad-spectrum arenavirus entry inhibitor. J. Virol. 82, 10768–10775.

Lee, A.M., Pasquato, A., Kunz, S., 2011. Novel approaches in anti-arenaviral drug development. Virology 411, 163–169.

Lee, A.M., Rojek, J.M., Spiropoulou, C.F., Gundersen, A.T., Jin, W., Shaginian, A., York, J., Nunberg, J.H., Boger, D.L., Oldstone, M.B., Kunz, S., 2008. Unique small molecule entry inhibitors of hemorrhagic fever arenaviruses. J. Biol. Chem. 283, 18734–18742.

Lee, K.J., Perez, M., Pinschewer, D.D., de la Torre, J.C., 2002. Identification of the lymphocytic choriomeningitis virus (LCMV) proteins required to rescue LCMV RNA analogs into LCMV-like particles. J. Virol. 76, 6393–6397.

Lestini, B.J., Goldsmith, K.C., Fluchel, M.N., Liu, X., Chen, N.L., Goyal, B., Pawel, B.R., Hogarty, M.D., 2009. Mcl1 downregulation sensitizes neuroblastoma to cytotoxic chemotherapy and small molecule Bcl2-family antagonists. Cancer Biol. Ther. 8, 1587–1595.

Lucas-Hourani, M., Dauzonne, D., Jorda, P., Cousin, G., Lupan, A., Helynck, O., Caignard, G., Janvier, G., Andre-Leroux, G., Khiar, S., Escriou, N., Despres, P., Jacob, Y., Munier-Lehmann, H., Tangy, F., Vidalain, P.O., 2013. Inhibition of pyrimidine biosynthesis pathway suppresses viral growth through innate immunity. PLoS Pathog. 9, e1003678.

Luthra, P., Naidoo, J., Pietzsch, C.A., De, S., Khadka, S., Anantpadma, M., Williams, C.G., Edwards, M.R., Davey, R.A., Bukreyev, A., Ready, J.M., Basler, C.F., 2018. Inhibiting pyrimidine biosynthesis impairs Ebola virus replication through depletion of nucleoside pools and activation of innate immune responses. Antivir. Res. 158, 288–302.

Madrid, P.B., Chopra, S., Manger, I.D., Gilfillan, L., Keepers, T.R., Shurtleff, A.C., Green, C.E., Iyer, L.V., Dilks, H.H., Davey, R.A., Kolokoltsov, A.A., Carrion Jr., R., Patterson, J.L., Bavari, S., Panchal, R.G., Warren, T.K., Wells, J.B., Moos, W.H., Burke, R.L., Tanga, M.J., 2013. A systematic screen of FDA-approved drugs for inhibitors of biological threat agents. PLoS One 8, e60579.

Mazur, S., Holbrook, M.R., Burdette, T., Joselyn, N., Barr, J., Pusl, D., Bollinger, L., Coe, L., Jahrling, P.B., Lackemeyer, M.G., Wada, J., Kuhn, J.H., Janosko, K., 2016. Safety precautions and operating procedures in an (A)BSL-4 laboratory: 2. General practices. J. Vis. Exp.(116). https://doi.org/10.3791/53600.

McCormick, J.B., Fisher-Hock, S.P., 2002. Lassa Fever. Springer-Verlag, Berlin, Heidelberg, New York.

Mendenhall, M., Russell, A., Juelich, T., Messina, E.L., Smee, D.F., Freiberg, A.N., Holbrook, M.R., Furuta, Y., de la Torre, J.C., Nunberg, J.H., Gowen, B.B., 2011a. T-705 (favipiravir) inhibition of arenavirus replication in cell culture. Antimicrob. Agents Chemother. 55, 782–787.

Mendenhall, M., Russell, A., Smee, D.F., Hall, J.O., Skirpstunas, R., Furuta, Y., Gowen, B.B., 2011b. Effective oral favipiravir (T-705) therapy initiated after the onset of clinical disease in a model of arenavirus hemorrhagic Fever. PLoS Neglected Trop. Dis. 5, e1342.

Meza-Avina, M.E., Wei, L., Liu, Y., Poduch, E., Bello, A.M., Mishra, R.K., Pai, E.F., Kotra, L.P., 2010. Structural determinants for the inhibitory ligands of orotidine-5'-monophosphate decarboxylase. Bioorg. Med. Chem. 18, 4032–4041.

Miranda, P.O., Cubitt, B., Jacob, N.T., Janda, K.D., de la Torre, J.C., 2018. Mining a krohnke pyridine library for anti-arenavirus activity. ACS Infect. Dis. 4, 815–824.

Mohr, E.L., McMullan, L.K., Lo, M.K., Spengler, J.R., Bergeron, E., Albarino, C.G., Shrivastava-Ranjan, P., Chiang, C.F., Nichol, S.T., Spiropoulou, C.F., Flint, M., 2015. Inhibitors of cellular kinases with broad-spectrum antiviral activity for hemorrhagic fever viruses. Antivir. Res. 120, 40–47.

Moreno, H., Gallego, I., Sevilla, N., de la Torre, J.C., Domingo, E., Martin, V., 2011. Ribavirin can be mutagenic for arenaviruses. J. Virol. 85, 7246–7255.

Nakanishi, T., Morokata, T., Kubo, K., Umeno, H., Eikyu, Y., Kozuki, Y., Seki, N., 2010. Effect of the inosine 5'-monophosphate dehydrogenase inhibitor BMS-566419 on rat cardiac allograft rejection. Int. Immunopharmacol. 10, 91–97.

Nguyen, M., Cencic, R., Ertel, F., Bernier, C., Pelletier, J., Roulston, A., Silvius, J.R., Shore, G.C., 2015. Obatoclax is a direct and potent antagonist of membrane-restricted Mcl-1 and is synthetic lethal with treatment that induces Bim. BMC Canc. 15, 568.

Nguyen, M., Marcellus, R.C., Roulston, A., Watson, M., Serfass, L., Murthy Madiraju, S.R., Goulet, D., Viallet, J., Belec, L., Billot, X., Acoca, S., Purisima, E., Wiegmans, A., Cluse, L., Johnstone, R.W., Beauparlant, P., Shore, G.C., 2007. Small molecule obatoclax (GX15-070) antagonizes MCL-1 and overcomes MCL-1-mediated resistance to apoptosis. Proc. Natl. Acad. Sci. U. S. A. 104, 19512–19517.

Ohmer, M., Weber, A., Sutter, G., Ehrhardt, K., Zimmermann, A., Hacker, G., 2016. Anti-apoptotic Bcl-XL but not Mcl-1 contributes to protection against virus-induced apoptosis. Cell Death Dis. 7, e2340.

Oppliger, J., Torriani, G., Herrador, A., Kunz, S., 2016. Lassa virus cell entry via dystroglycan involves an unusual pathway of macropinocytosis. J. Virol. 90, 6412–6429.

Osaki, S., Tazawa, H., Hasei, J., Yamakawa, Y., Omori, T., Sugiu, K., Komatsubara, T., Fujiwara, T., Sasaki, T., Kunisada, T., Yoshida, A., Urata, Y., Kagawa, S., Ozaki, T., Fujiwara, T., 2016. Ablation of MCL1 expression by virally induced microRNA-29 reverses chemoresistance in human osteosarcomas. Sci. Rep. 6, 28953.

Palacios, G., Druce, J., Du, L., Tran, T., Birch, C., Briese, T., Conlan, S., Quan, P.L., Hui, J., Marshall, J., Simons, J.F., Egholm, M., Paddock, C.D., Shieh, W.J., Goldsmith, C.S., Zaki, S.R., Catton, M., Lipkin, W.I., 2008. A new arenavirus in a cluster of fatal transplant-associated diseases. N. Engl. J. Med. 358, 991–998.

Panda, D., Das, A., Dinh, P.X., Subramaniam, S., Nayak, D., Barrows, N.J., Pearson, J.L., Thompson, J., Kelly, D.L., Ladunga, I., Pattnaik, A.K., 2011. RNAi screening reveals requirement for host cell secretory pathway in infection by diverse families of negative-strand RNA viruses. Proc. Natl. Acad. Sci. U. S. A. 108, 19036–19041.

Parker, W.B., 2005. Metabolism and antiviral activity of ribavirin. Virus Res. 107, 165–171.

Perez, M., Craven, R.C., de la Torre, J.C., 2003. The small RING finger protein Z drives arenavirus budding: implications for antiviral strategies. Proc. Natl. Acad. Sci. U. S. A. 100, 12978–12983.

Peters, C.J., 2002. Human infection with arenaviruses in the Americas. Curr. Top. Microbiol. Immunol. 262, 65–74.

Peters, C.J., 2006. Lymphocytic choriomeningitis virus–an old enemy up to new tricks. N. Engl. J. Med. 354, 2208–2211.

Pinschewer, D.D., Perez, M., Sanchez, A.B., de la Torre, J.C., 2003. Recombinant lymphocytic choriomeningitis virus expressing vesicular stomatitis virus glycoprotein. Proc. Natl. Acad. Sci. U. S. A. 100, 7895–7900.

Pushpakom, S., Iorio, F., Eyers, P.A., Escott, K.J., Hopper, S., Wells, A., Doig, A., Guilliams, T., Latimer, J., McNamee, C., Norris, A., Sanseau, P., Cavalla, D., Pirmohamed, M., 2019. Drug repurposing: progress, challenges and recommendations. Nat. Rev. Drug Discov. 18, 41–58.

Rathbun, J.Y., Droniou, M.E., Damoiseaux, R., Haworth, K.G., Henley, J.E., Exline, C.M., Choe, H., Cannon, P.M., 2015. Novel arenavirus entry inhibitors discovered by using a minigenome rescue system for high-throughput drug screening. J. Virol. 89, 8428–8443.

Raveh, A., Delekta, P.C., Dobry, C.J., Peng, W., Schultz, P.J., Blakely, P.K., Tai, A.W., Matainaho, T., Irani, D.N., Sherman, D.H., Miller, D.J., 2013. Discovery of potent broad spectrum antivirals derived from marine actinobacteria. PLoS One 8, e82318.

Regan, A.D., Whittaker, G.R., 2013. Entry of rhabdoviruses into animal cells. Adv. Exp. Med. Biol. 790, 167–177.

Rodrigo, W.W., de la Torre, J.C., Martinez-Sobrido, L., 2011. Use of single-cycle infectious lymphocytic choriomeningitis virus to study hemorrhagic fever arenaviruses. J. Virol. 85, 1684–1695.

Rojek, J.M., Sanchez, A.B., Nguyen, N.T., de la Torre, J.C., Kunz, S., 2008. Different mechanisms of cell entry by human-pathogenic Old World and New World arenaviruses. J. Virol. 82, 7677–7687.

Safronetz, D., Rosenke, K., Westover, J.B., Martellaro, C., Okumura, A., Furuta, Y., Geisbert, J., Saturday, G., Komeno, T., Geisbert, T.W., Feldmann, H., Gowen, B.B., 2015. The broad-spectrum antiviral favipiravir protects Guinea pigs from lethal Lassa virus infection post-disease onset. Sci. Rep. 5, 14775.

Samuel, S., Tumilasci, V.F., Oliere, S., Nguyen, T.L., Shamy, A., Bell, J., Hiscott, J., 2010. VSV oncolysis in combination with the BCL-2 inhibitor obatoclax overcomes apoptosis resistance in chronic lymphocytic leukemia. Mol. Ther. 18, 2094–2103.

Sintchak, M.D., Fleming, M.A., Futer, O., Raybuck, S.A., Chambers, S.P., Caron, P.R., Murcko, M.A., Wilson, K.P., 1996. Structure and mechanism of inosine monophosphate dehydrogenase in complex with the immunosuppressant mycophenolic acid. Cell 85, 921–930.

Sulkshane, P., Teni, T., 2017. BH3 mimetic Obatoclax (GX15-070) mediates mitochondrial stress predominantly via MCL-1 inhibition and induces autophagy-dependent necroptosis in human oral cancer cells. Oncotarget 8, 60060–60079.

Sykes, D.B., Kfoury, Y.S., Mercier, F.E., Wawer, M.J., Law, J.M., Haynes, M.K., Lewis, T.A., Schajnovitz, A., Jain, E., Lee, D., Meyer, H., Pierce, K.A., Tolliday, N.J., Waller, A., Ferrara, S.J., Eheim, A.L., Stoeckigt, D., Maxcy, K.L., Cobert, J.M., Bachand, J., Szekely, B.A., Mukherjee, S., Sklar, L.A., Kotz, J.D., Clish, C.B., Sadreyev, R.I., Clemons, P.A., Janzer, A., Schreiber, S.L., Scadden, D.T., 2016. Inhibition of dihydroorotate dehydrogenase overcomes differentiation blockade in acute myeloid leukemia. Cell 167, 171–186 e115.

Urata, S., Ngo, N., de la Torre, J.C., 2012. The PI3K/Akt pathway contributes to arenavirus budding. J. Virol. 86, 4578–4585.

Varghese, F.S., Rausalu, K., Hakanen, M., Saul, S., Kummerer, B.M., Susi, P., Merits, A., Ahola, T., 2017. Obatoclax inhibits alphavirus membrane fusion by neutralizing the acidic environment of endocytic compartments. Antimicrob. Agents Chemother. 61.

Vazquez-Calvo, A., Martin-Acebes, M.A., Saiz, J.C., Ngo, N., Sobrino, F., de la Torre, J.C., 2013. Inhibition of multiplication of the prototypic arenavirus LCMV by valproic acid. Antivir. Res. 99, 172–179.

Wang, Q.Y., Bushell, S., Qing, M., Xu, H.Y., Bonavia, A., Nunes, S., Zhou, J., Poh, M.K., Florez de Sessions, P., Niyomrattanakit, P., Dong, H., Hoffmaster, K., Goh, A., Nilar, S., Schul, W., Jones, S., Kramer, L., Compton, T., Shi, P.Y., 2011. Inhibition of dengue virus through suppression of host pyrimidine biosynthesis. J. Virol. 85, 6548–6556.

Welch, S.R., Guerrero, L.W., Chakrabarti, A.K., McMullan, L.K., Flint, M., Bluemling, G.R., Painter, G.R., Nichol, S.T., Spiropoulou, C.F., Albarino, C.G., 2016. Lassa and Ebola virus inhibitors identified using minigenome and recombinant virus reporter systems. Antivir. Res. 136, 9–18.

Wolff, S., Ebihara, H., Groseth, A., 2013. Arenavirus budding: a common pathway with mechanistic differences. Viruses 5, 528–549.

Xiang, W., Yang, C.Y., Bai, L., 2018. MCL-1 inhibition in cancer treatment. OncoTargets Ther. 11, 7301–7314.

York, J., Dai, D., Amberg, S.M., Nunberg, J.H., 2008. pH-induced activation of arenavirus membrane fusion is antagonized by small-molecule inhibitors. J. Virol. 82, 10932–10939.